# A Continuous Current Mode Boost Converter With Modified Flying Capacitor Lossless Snubber

Kyu-Min Cho Student Member
Ki-Bum Park Student Member
Yung-Do Kim Student Member
Gun-Woo Moon Member

KAIST
335, Gwahangno, Yuseong-Gu, Daejeon, 305-701, Republic of Korea
gwmooon@ee.kaist.ac.kr

***Abstract* -- A continuous current mode boost converter with modified flying capacitor lossless snubber is proposed in this paper. The proposed converter charges the flying capacitor using a coupled inductor without the help of the reverse recovery current. As a result, it can reduce switching loss and guarantee the wide snubber reset ranges. The operation principle, characteristics, and experimental results are presented to verify the feasibility of the proposed converter.**

***Index Terms*—Boost converter, flying capacitor passive lossless snubber, coupled inductor, wide snubber reset ranges.**

## I. INTRODUCTION

The continuous current mode (CCM) boost converter is a very attractive topology for high power applications because of its advantages such as low conduction loss, small EMI filter, and low current stress of semiconductor devices. Especially, it is widely used in the power factor correction (PFC) circuit because of its continuous input current and high DC conversion ratio. However, a large reverse recovery current of output rectifier, which occurs at main switch turn-on, creates a high current spike on the main switch. This high current spike causes not only high current stress but also high switching loss on the main switch. To overcome these drawbacks, various active and passive snubbers have been proposed [1]-[16].

Among them, active snubbers proposed in [1]-[3] can reduce the reverse recovery current by employing the auxiliary switch. Before the main switch is turned on, the auxiliary switch shifts the output diode current to a new parallel branch. As a result, the output diode is turned off with zero current condition. Furthermore, it can achieve zero voltage switching (ZVS) of main switch using the energy of the additional resonant inductor. However, the auxiliary switch is turned on while its drain-source voltage is equal to the output voltage, and it is turned off while its current is greater than the boost inductor current. Therefore, the auxiliary switch operates under hard switching conditions, which results in high switching losses. Active snubbers proposed in [4]-[8] can achieve ZVS of main and auxiliary switches by adopting active clamp circuit. However, they require an isolation gate driver and overlapping gate signals of the main and auxiliary switches. It causes high cost and complexity of control circuit. Especially, overlapping gate signals will lead to a fatal circuit failure.

To achieve low cost, simple control circuit, and high reliability, passive lossless snubbers use passive components instead of an auxiliary active switch [9]-[16]. Generally, they can be divided into coupled inductor type and flying capacitor type. The coupled inductor lossless snubber proposed in [10] can easily shift the output diode current to a new parallel branch using coupled inductor. However, due to the leakage inductor by the coupled inductor, it has severe, undesirable voltage ringing on the auxiliary diode. Thus, the extra clamping circuit is mandatory in the practical applications to protect the devices. The coupled inductor lossless snubbers proposed in [12], [13] can achieve low voltage stress of all semiconductor devices by adopting additional diodes. However, additional diodes causes extra conduction loss occurs when main switch on or off period.

The flying capacitor lossless snubber proposed in [14]-[16] features a simple structure, low voltage stress of semiconductor devices, and low additional conduction loss due to the auxiliary diodes. It utilizes snubber inductor as the turn-on current snubber, and one flying capacitor and two auxiliary diodes as the reset network. When main switch is turned on, the reverse recovery energy is stored in the snubber inductor. After that, it is delivered to the flying capacitor at the output diode turn-off. This energy is then used to reset the snubber inductor after the main switch is turned off. However, if the energy stored in the flying capacitor is insufficient, the output diode can not be turned on and a large reverse recovery current occurs due to two auxiliary diodes. Therefore, a trade-off should be required between the value of snubber inductor and the peak reverse recovery current, i.e. as the snubber inductor is increased, it can reduce the switching loss related with the reverse recovery but it has narrow

978-1-4244-5287-3/10/$26.00 ©2010 IEEE

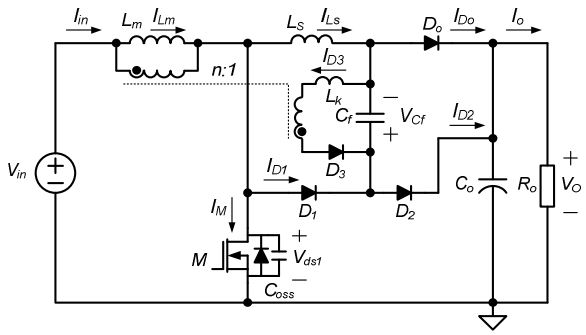


Fig. 1 Circuit diagram of proposed converter

snubber reset ranges. This snubber reset characteristics of the flying-capacitor lossless snubber makes it difficult to design the snubber inductor especially when it is applied to the applications with wide input ranges such as a PFC boost converter.

This paper proposes a new CCM boost converter with modified flying capacitor lossless snubber. As shown in Fig. 1, the proposed converter has a new branch that consists of a coupled inductor and a auxiliary diode $D_3$ compared to the conventional flying capacitor lossless snubber. When the main switch M is turned on, the voltage $V_{Cf}$ across flying capacitor is charged to $2V_{in}/n$ through a new branch without the help of the reverse recovery current. Therefore, it can effectively reduce the reverse recovery current which is required to charge the flying capacitor maintaining wide snubber reset ranges.

## II. Operational Principles

Fig. 2 and Fig. 3 show key operational waveforms and topological stages of the proposed converter, respectively. To analyze the steady-state operation conveniently, the coupled inductor is regarded as a combination of the magnetizing inductor $L_m$, an ideal transformer with the turns ratio n : 1 (n>1) and a leakage inductor $L_k$. In addition, the magnetizing current $I_{Lm}$ is assumed to be constant in one switching period. One switching period is divided into eight modes and each mode is explained as follows.

Mode 1 [$t_0$~$t_1$]: Switch M is off-state, diode $D_o$ is forward-biased, and the magnetizing current $I_{Lm}$ is transferred from input to output. Meanwhile diodes $D_1$, $D_2$ and $D_3$ are reverse-biased, and the flying capacitor voltage $V_{Cf}(t)$ is zero.

Mode 2 [$t_1$~$t_2$]: At time $t_1$, switch M is turned on. The output voltage $V_o$ is applied to the snubber inductor $L_S$ and the magnetizing current $I_{Lm}$ begins to commutate from diode $D_o$ to switch M. Concurrently, the flying capacitor $C_f$ begins to be charged through the coupled inductor and diode $D_3$. In this mode, the snubber inductor current $I_{Ls}(t)$, the current $I_{D3}(t)$ flowing through diode $D_3$, and the flying capacitor voltage $V_{Cf}(t)$ can be expressed as follows:

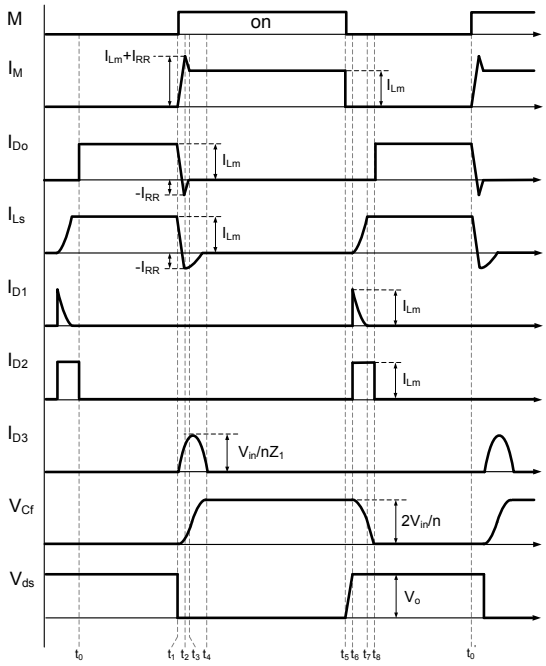


Fig. 2 Key operational waveforms.

$$I_{Ls}(t) = I_{Lm} - \frac{V_o}{L_s}(t - t_1). \quad (1)$$

$$I_{D3}(t) = \frac{V_{in}}{nZ_1}\sin(\omega_1(t - t_1)). \quad (2)$$

$$V_{Cf}(t) = \frac{V_{in}}{n}(1 - \cos(\omega_1(t - t_1)), \quad (3)$$

where $Z_1 = \sqrt{L_k / C_f}$ and $\omega_1 = \sqrt{L_k C_f}$.

When $I_{Ls}(t)$ is equal to zero, the magnetizing current $I_{Lm}$ completely commutates to the switch M. However, $I_{Ls}(t)$ decreases $-I_{RR}$ due to reverse-recovery charge of diode $D_o$.

Mode 3 [$t_2$~$t_3$]: At time $t_2$, diode $D_o$ is turned off at the peak of the reverse recovery current $-I_{RR}$. Since diode $D_o$ is reverse-biased, the reverse recovery current of $L_s$ creates resonance path $L_s$-$D_1$-$C_f$. In this mode, the snubber inductor current $I_{Ls}(t)$ can be expressed as follows:

$$I_{Ls}(t) = I_{RR}\cos(\omega_2(t - t_2)) \quad \text{and} \quad \omega_2 = \sqrt{L_s C_S}. \quad (4)$$

Mode 4 [$t_3$~$t_4$]: At time $t_3$, diode $D_o$ is turned off at the peak of the reverse recovery. Since $V_{in}$ is still applied to the primary of ideal transformer, $V_{Cf}(t)$ is increased by the half-period resonance between $L_k$ and $C_f$.

Mode 5 [$t_4$~$t_5$]: At time $t_4$, the half-period resonance between $L_k$ and $C_f$ is finished and diode $D_3$ is turned off. After this mode, $V_{Cf}(t)$ is maintained with its peak value $2V_{in}/n$.

Mode 6 [$t_5$~$t_6$]: At time $t_5$, switch M is turned off. Since $L_m$+$L_S$ is large enough to be considered as a current source, the drain-source voltage $V_{ds1}(t)$ of switch M is linearly increased as follows:

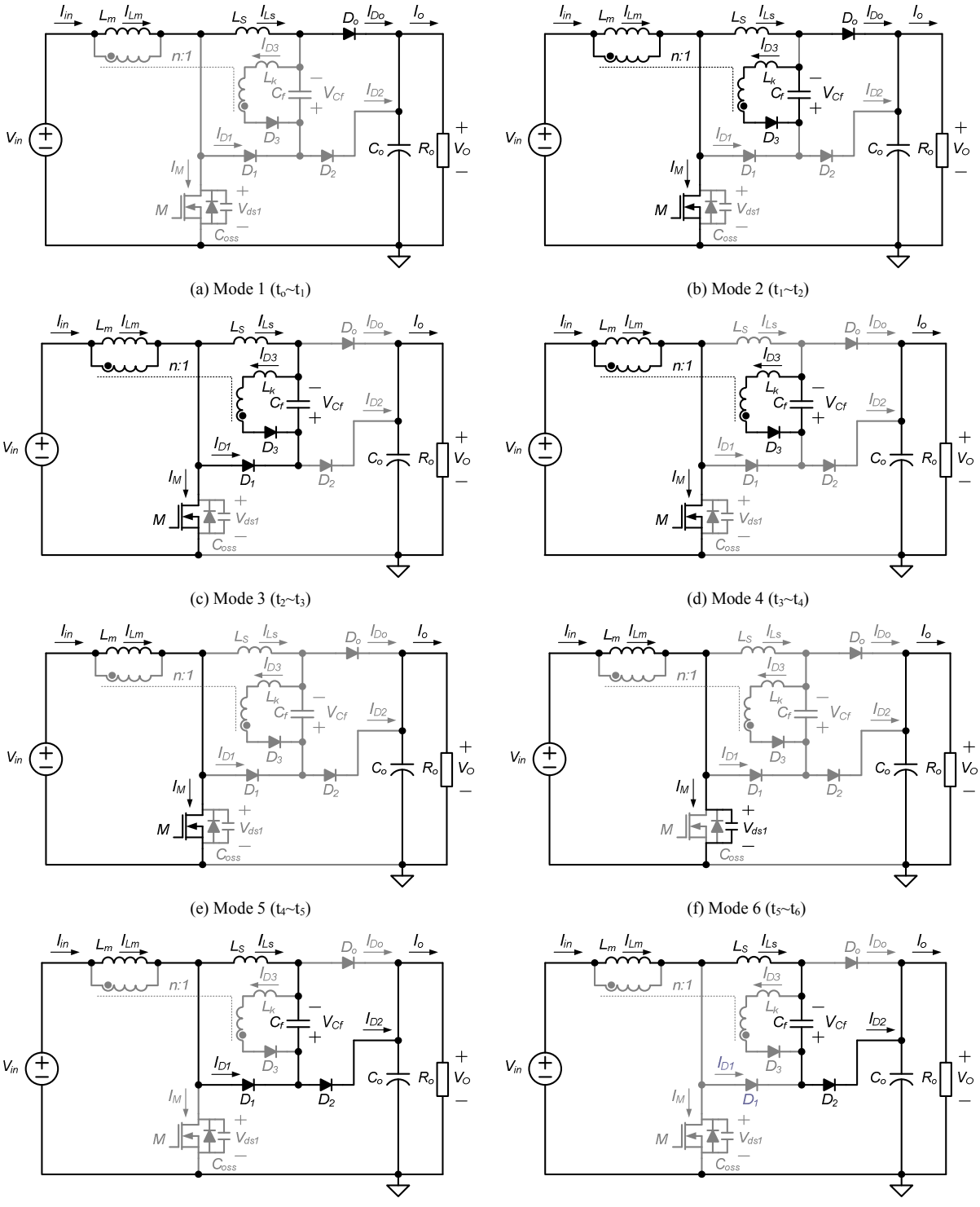


(a) Mode 1 ($t_0$~$t_1$)

(b) Mode 2 ($t_1$~$t_2$)

(c) Mode 3 ($t_2$~$t_3$)

(d) Mode 4 ($t_3$~$t_4$)

(e) Mode 5 ($t_4$~$t_5$)

(f) Mode 6 ($t_5$~$t_6$)

(g) Mode 7 ($t_6$~$t_7$)

(h) Mode 8 ($t_7$~$t_8$)

Fig. 3 Topological stages

$$V_{ds1}(t) = \frac{I_{Lm}}{C_{oss}}(t - t_5) . \quad (5)$$

Mode 7 [$t_6$~$t_7$]: At time $t_6$, $V_{ds1}(t)$ reaches $V_o$ and diodes $D_1$ and $D_2$ are turned on. Since diode $D_1$ is turned on, $V_{Cf}(t)$ is applied to $L_s$. In this mode, $I_{Ls}(t)$ and $V_{Cf}(t)$ can be expressed as follows:

$$I_{Ls}(t) = \frac{2V_{in}}{nZ_2}\sin(w_2(t - t_6)) . \quad (6)$$

$$V_{C_f}(t) = \frac{2V_{in}}{n}\cos(w_2(t - t_6)) , \quad (7)$$

where $Z_2 = \sqrt{L_S / C_f}$ .

To reset the snubber inductor, $2V_{in}/nZ_2$ must be greater than $I_{Lm}$. Otherwise, it has high switching loss due to two diodes $D_{1,2}$ and circuit parasitic inductance. At the end of this mode, $I_{Ls}(t)$ becomes $I_{Lm}$ and diode $D_1$ is turned off.

Mode 8 [$t_7$~$t_8$]: At time $t_7$, $I_{Lm}$ flows through $C_C$ and $D_2$. Since the $L_m$ is large enough to be considered as a current source, $V_{Cf}(t)$ is linearly decreased as follows:

$$V_{C_f}(t) = \sqrt{\left(\frac{2V_{in}}{n}\right)^2 - \frac{L_S I_{Lm}^2}{C_f}} - \frac{I_{Lm}}{C_f}(t - t_6) \quad (8)$$

At the end of this mode, $V_{Cf}(t)$ reaches zero, diode $D_2$ is turned off, and diode $D_o$ is turned on.

## III. CHARACTERISTICS

A. DC conversion ratio

To calculate the DC conversion ratio, $P_{in}$ and $P_o$ can be expressed as in (9) and (10), respectively.

$$P_{in} = \frac{V_{in}}{T_S}\left[\int_0^{T_S} I_{Lm}dt + \frac{1}{n}\int_{t_1}^{t_1+\frac{\pi}{\omega_1}} \frac{V_{in}}{nZ_1}\sin(\omega_1(t - t_1))dt\right] . \quad (9)$$

$$P_o = V_o I_o = \frac{V_o^2}{R_o} = V_o \frac{I_{Lm}}{1 - D} , \quad (10)$$

where $T_S$ is the switching period, $I_o$ is the load current, and $R_o$ is the load resistance.

From (9) and (10), the DC conversion ration can be obtained as follows:

$$\frac{V_o}{V_{in}} = \frac{1}{2(1 - D)} + \sqrt{\frac{1}{4(1 - D)^2} + \frac{R_o C_C}{n^2 T_S}} . \quad (11)$$

Fig. 4 shows the DC conversion ratio according to the variations of load conditions with n=10. As can be seen in (11), the constant energy is transferred from the input for charging the clamping capacitor. Therefore, as load is decreased, the proposed converter has higher DC conversion ratio compared to that of the conventional boost converter.

B. Transformer turns ratio

The transformer turn ratio n is related with the reset ranges of $L_s$ and the voltage stress of $D_o$. As n is decreased, it can achieve wide reset ranges due to high peak value of $V_{Cf}$. However, this high peak value of $V_{Cf}$ causes high voltage

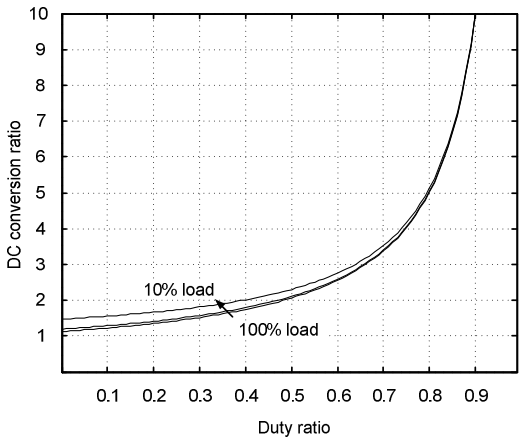


Fig. 4 DC conversion ratio according to load conditions when n=10

stress of $D_o$ as follows:

$$V_{D_O,\max} = V_o + \frac{2V_{in,\max}}{n} . \quad (12)$$

C. Snubber inductor and flying capacitor

To effectively reduce the reverse recovery current, two conditions should be satisfied. First, the turn-off rate of $I_{Do}$ should be less than less than 100A/μs. Since the output voltage $V_o$ is 400V, it is known from (1) that the snubber inductor $L_s$ should be more than 4μH. Second, the snubber inductor current $I_{Ls}(t)$ should be larger than $I_{Lm}$ at $t_7$, i.e. the energy stored in the flying capacitor should be larger than the energy stored in the snubber inductor with $I_{Lm}$. From (3) and (5), the flying capacitor can be obtained as follows:

$$C_f > \frac{nL_s I_{Lm}}{2V_{in}} . \quad (13)$$

D. Reverse recovery current

Fig. 5 shows the reverse recovery current of the conventional converter and proposed converter, respectively. For the conventional converter, it requires large reverse recovery current to charge the flying capacitor. This large reverse recovery current causes high current stress and high turn-on switching loss on the main switch. In addition, the reverse recovery current is the function of the diode characteristics, the forward current through diode at the main switch turn-on and the slope of the diode turn-off current. As a result, determining the reverse recovery current from manufacturer data is unreliable because they often provide a limited number of operation points. Therefore, the snubber inductor should be determined experimentally.

On the other hand, the proposed converter can charge the flying capacitor using the auxiliary circuit regardless of the reverse recovery current. Therefore, it features low current stress of the main switch, low switching loss, and wide snubber reset ranges.

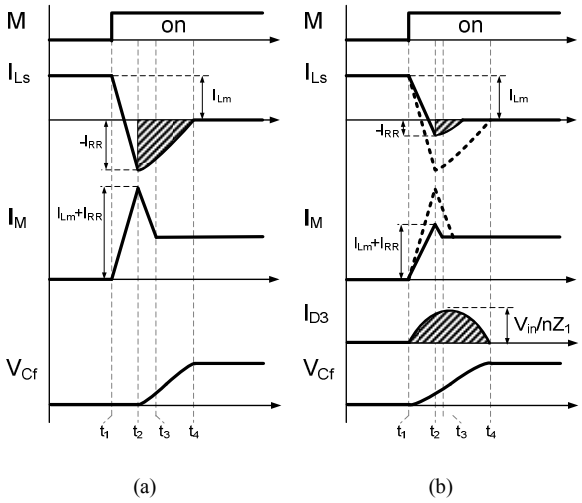


Fig. 5. Reverse recovery current.
(a) Conventional converter (b) Proposed converter

## IV. EXPERIMENTAL RESULTS

To verify the feasibility of the proposed converter, a 700W CCM PFC boost converter incorporated with the proposed snubber is implemented with following specifications: input voltage: $V_{in}$=90$V_{rms}$~265$V_{rms}$, output voltage: $V_o$=400V, switching frequency: $f_s$=65kHz, boost inductor: $L_m$=645μF, turn ratio of boost inductor: n:1=10:1, main switch: M=SPP20N60C3 x 2 in parallel, diodes $D_1$, $D_2$, $D_3$, and $D_o$=RHRP1560, flying-capacitor: $C_f$=940nF, snubber inductor: $L_s$=5μH.

Fig. 6 shows the input voltage and input current of the proposed converter at $V_{in}$=110$V_{rms}$ and $V_{in}$=220$V_{rms}$, respectively. As shown in this figure, it can be seen that the unity power factor is well achieved.

Fig. 7 shows the key experimental waveforms of the proposed converter at $V_{in}$=110$V_{rms}$ and $V_{in}$=220$V_{rms}$, respectively. Since the flying capacitor voltage $V_{Cf}$ is charged by the coupled inductor, the proposed converter can effectively reduce the reverse recovery current compared to the conventional boost converter with flying capacitor snubber. In addition, diode $D_2$ is turned off before the main switch is turned on with the help of the high as shown in Fig. 7 (b) and (d). As a result, wide snubber reset ranges can be achieved.

Fig. 8 shows the comparative measured efficiency according the load and input voltage variations. The proposed snubber shows the higher efficiency over the entire load conditions. Especially, it can achieve high efficiency when the input voltage is low, i.e. large reverse recovery current occurs.

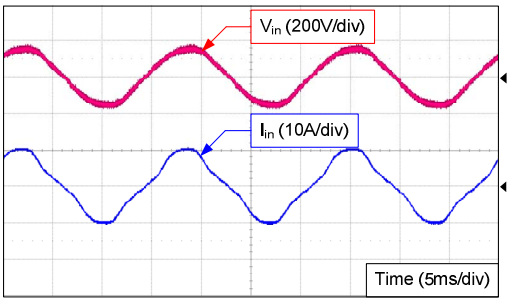


(a)

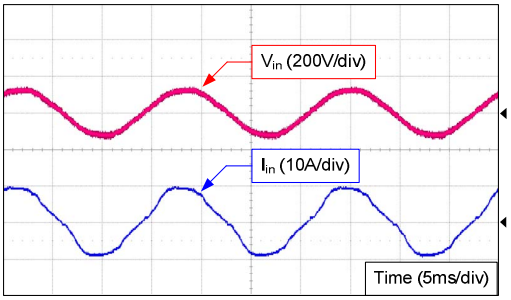


(b)

Fig. 6 Input voltage and input current.
(a) $V_{in}$ and $I_{in}$ at $V_{in}$=110$V_{rms}$ (b) $V_{in}$ and $I_{in}$ at $V_{in}$=220$V_{rms}$

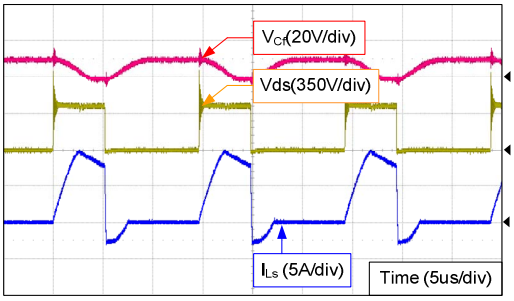


(a) $V_{Cf}$, Vds, and $I_{Ls}$ at $V_{in}$=110$V_{rms}$

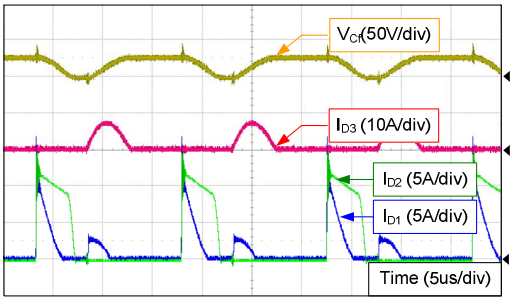


(b) $V_{Cf}$, $I_{D1}$, $I_{D2}$, and $I_{D3}$ at $V_{in}$=110$V_{rms}$

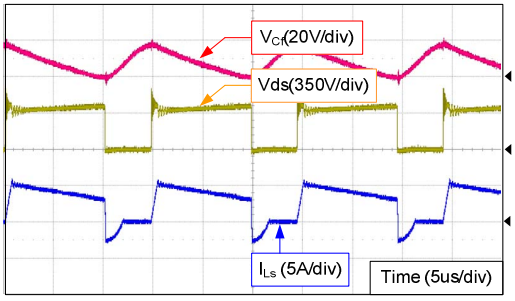


(c) $V_{Cf}$, Vds, and $I_{Ls}$ at $V_{in}$=220$V_{rms}$

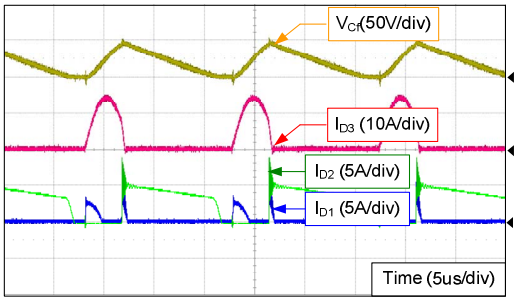


(d) $V_{Cf}$, $I_{D1}$, $I_{D2}$, and $I_{D3}$ at $V_{in}$=220$V_{rms}$

Fig. 7 Key experimental waveforms.

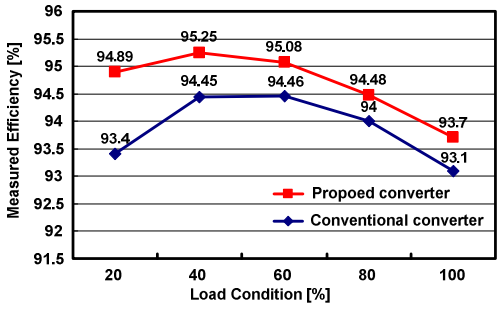


(a)

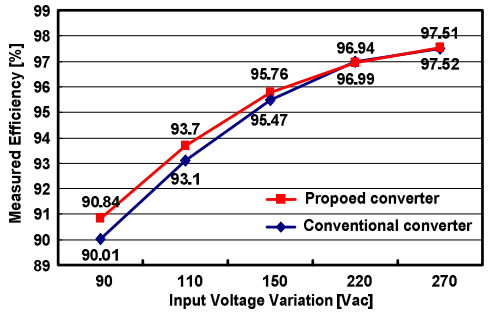


(b)

Fig. 8 Measured efficiency.
(a) Measured efficiency according to load variation at $V_{in}$=110$V_{rms}$.
(b) Measured efficiency according to input variation at 100% load.

## V. CONCLUSION

This paper proposes a new CCM boost converter with modified flying capacitor lossless snubber. The proposed converter charges the flying capacitor by adopting simple auxiliary circuits. As a result, it can reduce the reverse recovery which is required to charge the flying capacitor, and switching loss related with the reverse recovery current. Experimental result of 700W prototype shows that the proposed converter is suitable for the CCM boost converter.

## REFERENCES

[1] R. Streit and D. Tollik, "High efficiency telecom rectifier using a novel soft-switched boost-based input current shaper," in Proc. INTELEC,91 Ann. Meet., pp.720-726.
[2] G. Hua, C.S. Leu, and F.C. Lee, "Novel zero-voltage-transition PWM converter," in Proc. IEEE PESC'92 Ann. Meet., pp.55-61.
[3] D.C. Martins, F.J. M. de Sexias, J.A. Brilhante, and I. Barbi, "A family of dc-to-dc PWM converters using a new ZVS commutation cell," in Proc. IEEE PESC'93 Ann. Meet., pp.524-530.
[4] J. Bassett, "New, zero voltage switching, high frequency boost converter topology for power factor correction," in Proc. INTELEC'95 Ann. Meet., pp.813-820.
[5] C.M.C. Duarte and I. Barbi, "A new family of ZVS-PWM active-clamping dc-to-dc boost converters: Analysis, design, and experimentation," in Proc. INTELEC'96 Ann. Meet., pp.305-312.
[6] M. M. Jovanovic, "A technique for reducing rectifier reverse-recoverry-related losses in high-voltage, high-power boost converters," in Proc. IEEE APEC'97 Ann. Meet., pp.1000-1007.
[7] C.M.C. Duarte and I. Barbi,"An improved family of ZVS-PWM active clamping dc-to-dc converters," in Proc. IEEE IAS'84 Ann. Meet. Pp.669-675.
[8] Milan M. Jovanovic and Youngtaek Jang, "A new, soft-switching boost converter with isolated active snubber," in Proc. IEEE IAS'84 Ann. Meet., pp.860-867.
[9] J.A. Lambert, J.B. Vieira, L.C. Freitas, L.R. Barbosa, and B.J. Farias, "A boost PWM soft-single-switched converter with low voltage and current streeses," in IEEE Trans. Power Elec. Vol. 13, No. 1, Jan. 1998, pp.26-35.
[10] P.J.M. Menegaz, J.L.F. Viera and D.S.L. Simonetti, "A magnetically coupled regererative turn-on and turn-off snubber configuration," in IEEE Trans. Ind. Elec., Vol 47, No.4. Aug. 2000, pp.722-728.
[11] Q. Zhao, F.F. Tao, P. Xu, J. Wei, and F.C. Lee, "Improving performance of continuous current mode boost converter for power factor correction," in Proc. Center for Power Electronics Annual Seminar, 2000, pp.282-287.
[12] D.D.C Lu, D.K. Cheng, and Y.S. Lee, "A single-switch continuous conduction mode boost converter with reduced reverse recovery and switching losses", in IEEE Trans. Ind. Elec. Vol.50, No. 4, Aug. 2003. pp. 767-776.
[13] W. Dong, Q. Zhao, J. Liu, and F.C. Lee, "A boost converter with lossless snubber under minimum voltage stress," in Proc. IEEE APEC'02, Ann. Meet. Pp.509-515.
[14] H. Levy, I. Zafrany, G. Ivensky and S. Ben-Yaakov, "Analysis and evaluation of a lossless turn-on snubber," in Proc. IEEE APEC'97. pp.757-763.
[15] A. Pietkiewicz and D. Tollik, "Snubber circuit and mosfet paralleling considerations for high power boost-based power factor correctors," in Proc. IEEE INTELEC'95, pp.41-45.
[16] I. D. Jitaru, "Soft transitions power factor correction circuit," in Proc. IEEE HFPC'93, pp.41-45.